Supporting Information

Enhanced autophagy contributes to protective effects of IL-22 against acetaminophen-induced liver injury

Ruidong Mo[1,2#], Rongtao Lai[1,2#], Jie Lu[1,2#], Yan Zhuang[1],Tianhui Zhou[1,2], Shaowen Jiang[1,2], Peipei Ren[1,2], Ziqiang Li[1,2], Zhujun Cao[1,2], Yuhan Liu[1,2], Lichang Chen[1,2], Lifu Xiong[1,2], Peng Wang[1,2], Hui Wang[1], Wei Cai[1], Xiaogang Xiang[1,2*], Shisan Bao[3*], Qing Xie[1,2*]

[1]Department of Infectious Diseases, [2]Translational Lab of Liver Diseases, Ruijin Hospital, Shanghai Jiao Tong University School of Medicine, Shanghai, China

[3]Discipline of Pathology, School of Medical Sciences and Bosch Institute, Charles Perkins Centre, The University of Sydney, New South Wales 2006, Australia

[#]These authors contributed equally to this work.

[*]Address correspondence to Qing Xie, xieqingrjh@163.com, Shisan Bao, bob.bao@sydney.edu.au, or Xiaogang Xiang, shine-xxg@163.com

Table of contents

Supplementary materials and methods

Reagents

APAP and chloroquine were purchased from Sigma-Aldrich (St. Louis, MO, USA). Dorsomorphin (compound C) was purchased from Selleck Chemicals (Houston, TX, USA).

Biochemical and histological assessment

Serum alanine aminotransferase (ALT) and aspartate aminotransferase (AST) activities were determined as described previously [1]. Liver tissues were fixed in 4% paraformaldehyde, then embedded in paraffin, and sectioned at 5 μm for H&E staining. The necrotic areas in liver tissue were quantified by Image J 1.50 software [2].

Measurement of hepatic reactive oxygen species (ROS)

The collected liver tissues were immediately embedded in tissue-freezing medium (O.C.T compound, Tissue-Tek, CA, USA) and stored at -80^{o}C. Frozen sections were cut at 8 μm thickness on a Leica CM1900 cryotome. Hepatic ROS was detected using CM-H2DCFDA (Genmed Scientific Inc, USA). The images of the sections were captured on a Leica DM 4000B LED photomicroscope with fluorescent microscopy (490nm excitation, 520 nm emission).

TUNEL staining

The frozen sections were labeled for TUNEL staining [3], according to the instruction from the manufacturer (Roche, Switzerland).

Inflammatory cytokines quantification in serum

Serum levels of IL-6 and TNF were determined using cytokine bead array (CBA, BD Biosciences, MA, USA) [4]. Serum levels of IL-22 were measured using ELISA kit (R&D, M2200, MN, USA) [5] following the instruction from the manufacturer.

Quantitative Real-Time PCR (qRT-PCR) and RT^2 Profiler PCR Array

Total RNA was extracted from mice liver tissues with Trizol (Invitrogen, Carlsbad, CA), as previously described [6]. The PCR array of oxidative stress, inflammatory and autophagy related genes transcript expression was determined by RT^2 Profiler PCR Array (MS-PA-cus-118, BioTNT Biosciences Inc., Shanghai, China) [7]. cDNA was synthesized using oligo (dT) primers (Takara, Dalian, China), qRT-PCR was performed on the ABI ViiA7 (Applied Bio systems, Foster, CA) following the manufacturer's instructions. The primers listed in **Supplementary Table 1** were purchased from Sangon Biotech Co., Ltd (Shanghai, China). Relative mRNA levels were normalized to GAPDH, the expression differences were determined by the $2^{-\Delta\Delta}$ CT method. Each lysate was performed three times and each time in triplicates.

Transmission electron microscopy (TEM)

Liver tissues were fixed with 2.5% glutaraldehyde in phosphate buffer, washed and

fixed in 1% OsO4, then dehydrated through graded ethanol solutions and embedded in Spurr resin. The sections (70 nm) were counterstained with uranyl acetate and lead citrate. Electron microscopy was performed by TEM (Philips, CM120) [8].

Immunohistochemistry

Immunohistochemistry was performed as previously described [9]. The liver sections were labeled with rabbit anti mouse LC3 antibody (Abgent, San Diego, CA, USA, 1:50), Ki-67 (Abcam, Cambridge, MA, USA, 1:50) or PCNA antibody (Abcam, Cambridge, MA, USA, 1:800) followed by secondary antibody (Peroxidase AffiniPure Goat Anti-Rabbit IgG (H+L), Jackson ImmunoResearch, PA, USA) according to the manufacturer's instructions. The labeled sections were examined under the Leica DM 4000B LED photomicroscope.

Cell culture and transfection using GFP-LC3

Human non-tumor hepatic L02 cells, obtained from Type Culture Collection of Chinese Academy of Sciences (Shanghai, China) [10], were cultured in RPMI 1640 supplemented with 10% [v/v] fetal bovine serum, 2mM glutamine at 37℃ with 95% air and 5% CO_2.

Green fluorescent protein and LC3 (GFP-LC3) fusion protein is a reliable indicator of autophagy initiation by the examination of LC3 puncta or dots [11]. L02 cells were transfected with pBABE-puro mCherry-EGFP-LC3B (Addgene plasmid # 22418, a gift from Dr. Zhiqun Song, Shanghai Jiao Tong University) [12], the transfection was

performed by lipofectamine 3000 (Life Technologies, CA, USA). GFP-LC3 expressing L02 cells were exposed to different treatment, then cellular fluorescent levels were measured to reflect autophagy activity. The transfected L02 cells were treated with IL-22 (400 ng/ml) for 1 hour [13], followed by treatment with APAP (5 mM) for 6 hours, then the cellular GFP-LC3 dots was evaluated, using a Zeiss fluorescence microscope (LSM 710).

Isolation and culture of primary mouse hepatocytes

Primary hepatocytes were isolated from the mice as previously described [14]. Briefly, C57BL/6J male mice were anesthetized with 10% chloral hydrate, and the livers were perfused with collagenase (Gibco, MA, USA) (0.05% in Hank's solution) through portal vein [14]. The perfused liver was transferred into collagenase solution to further release the dispersed cells for 10 min in the plate. The suspension was filtered through a 100 μm membrane and washed three times. Hepatocytes pellets were suspended in hepatocyte medium (Sciencecell, 5201, CA, USA) containing 10% fetal bovine serum (Gibco, MA, USA) after aspiration of the supernatant. Then hepatocytes were seeded onto type I collagen-coated dish (4×10^4 cells/cm^2) in hepatocyte medium.

Cell viability assay

Cell viabilities were determined using 3-(4,5-dimethylthizaol-2-yl)-2, 5-diphenyltetrazolium bromide (MTT) assay kit (Beyotime, Nantong, China). L02 cells were treated with IL-22 (400 ng/ml) for 1 hours, then APAP (5 mM) for 24 hours.

MTT solutions was added into the plates and allowed to incubate for 4 hours. The formazan in cells was dissolved in 10% SDS-5% iso-butanol-0.01M HCL, the absorbance was measured at 570 nm.

Assessment of lactate dehydrogenase (LDH) activity

LDH released in the culture medium can reflect the amount of cells death [15]. The levels of LDH were detected using a commercial kit (Beyotime, Nantong, China).

Western blot analysis

Briefly, extracted total proteins were quantified using bicinchoninic acid method. The following primary antibodies were used in western blot: p-JNK (Thr183/Thr185) (Cat. No 4668), JNK (Cat. No 9252), p-AMPK (Thr172) (Cat. No 4188), AMPK (Cat. No 2603), p-STAT3 (Tyr705) (Cat. No 9145), STAT3 (Cat. No 4904), SQSTM1/p62 (Cat. No 5114) (Cell Signaling Technology Inc. Danvers, MA, USA), LC3 (L7543, Sigma-Aldrich, St. Louis, MO, USA), GAPDH (AG019, Beyotime, Nantong, China). Goat anti-rabbit IgG-HRP (Cell Signaling Technology, MA, USA) and goat anti-mouse IgG-HRP (Beyotime, Nantong, China) were used as secondary antibodies. The proteins were detected using ECL detection reagent (New Cell & Molecular Biotech, Shanghai, China).

Statistical analysis

Statistical analyses were performed, using the Graph Prism 6.01 (San Diego, CA,

USA). Data were expressed as mean ± SEM. Comparisons between two groups were performed using unpaired t test or the Mann-Whitney U test, among three groups using ANOVA test or Kruskal-Wallis test where appropriate. *P* value less than 0.05 was considered statistically significant.

Supplementary Table 1

Supplementary Table 1. The mouse primer sequences for Real-Time quantitative PCR

Primer Name		Primer Sequences (5'-3')
GAPDH	Forward primer	AGGTCGGTGTGAACGGATTTG
	Reverse primer	TGTAGACCATGTAGTTGAGGTCA
IL-6	Forward primer	CACATGTTCTCTGGGAAATCGTGGA
	Reverse primer	TCTCTCTGAAGGACTCTGGCTTTGT
TNF	Forward primer	CCCTCACACTCAGATCATCTTCT
	Reverse primer	GCTACGACGTGGGCTACAG
IL-1β	Forward primer	GCAACTGTTCCTGAACTCAACT
	Reverse primer	ATCTTTTGGGGTCCGTCAACT
p62	Forward primer	AGAATGTGGGGGAGAGTGTG
	Reverse primer	TCTGGGGTAGTGGGTGTCAG
IL-22	Forward primer	GCTGCCTGCTTCTCATTGC
	Reverse primer	AAGGTGCGGTTGACGATGTA

Supplementary Figures

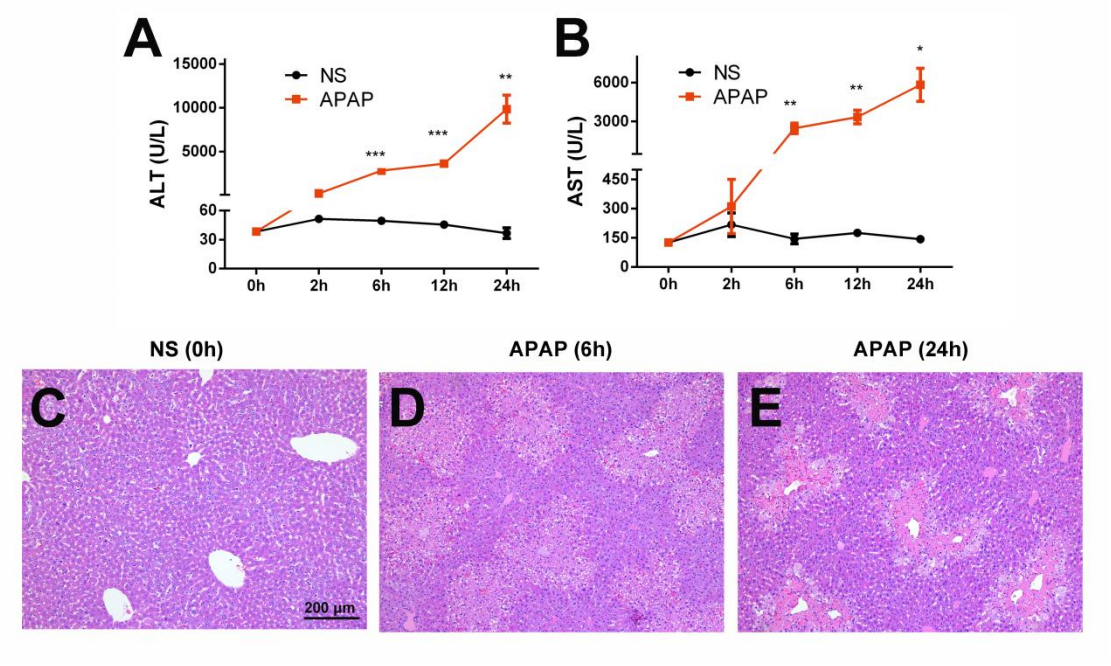

Supplementary Figure 1. Acetaminophen overdose-induced liver injury in mice. (A, B) Serum ALT and AST in mice were measured at various time points post-APAP challenged. (C, D, E) Representative images of mice liver H&E sections at 6 and 24 h after APAP treatment (original magnification 100×). Data are presented as means ± SEM, *p* value was calculated by Mann-Whitney test in A and B, **p* < 0.05, ***p* < 0.01 and ****p* < 0.001.

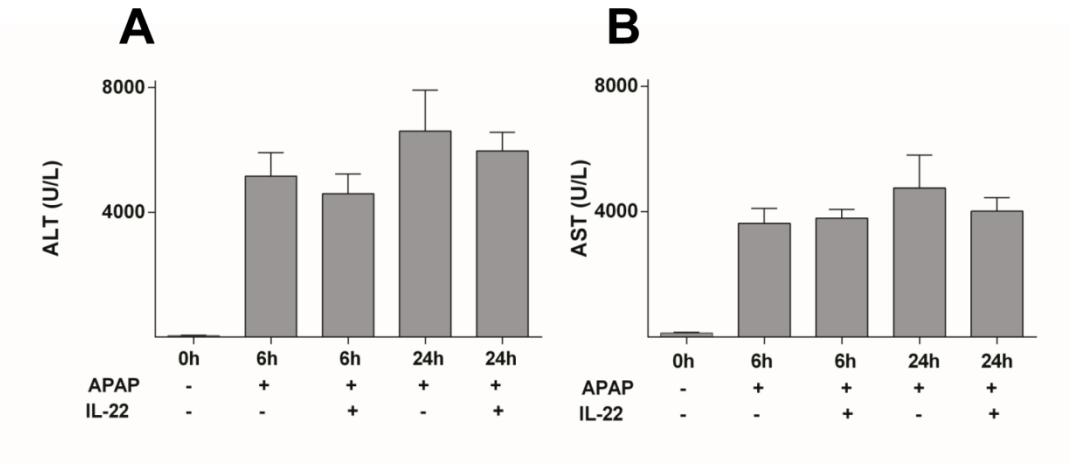

Supplementary Figure 2. Therapeutic IL-22 administration did not significantly alleviate liver injury induced by APAP.

(A, B) Serum ALT and AST from normal control, APAP-challenged and therapeutic IL-22 administration (2 h after APAP challenged) mice at 6 h and 24 h. Data are expressed as mean ± SEM.

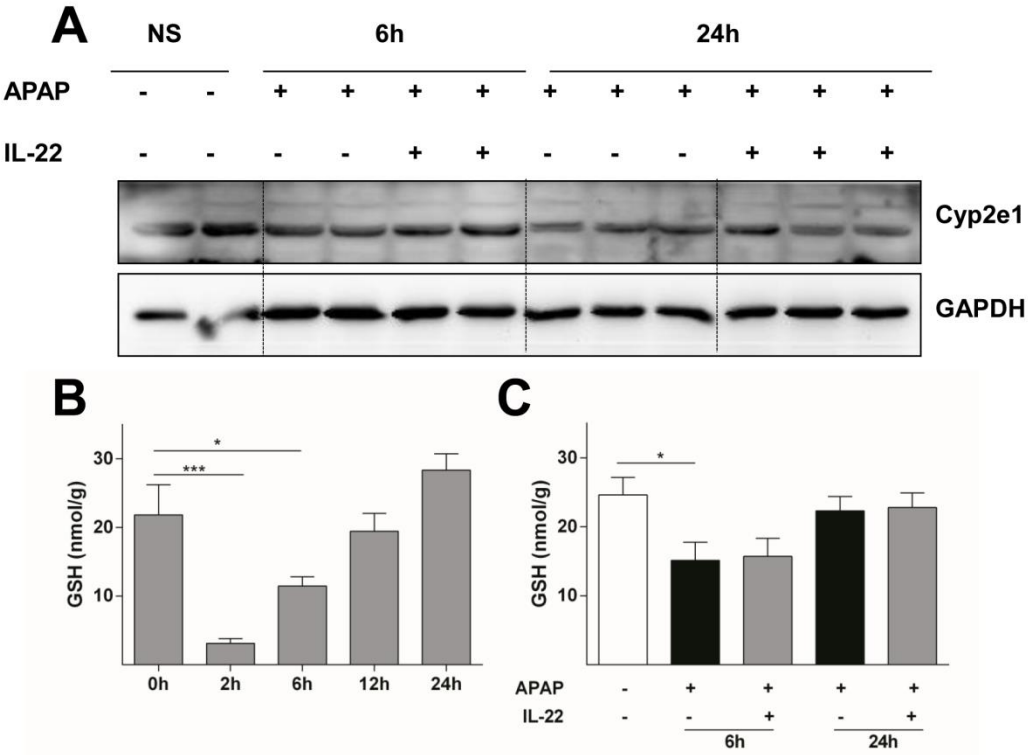

Supplementary Figure 3. IL-22 pretreatment did not alter hepatic APAP metabolism in mice challenged with APAP.

(A) Immunoblot analysis of hepatic CYP2E1 expression in the control (saline), APAP (400 mg/kg) and IL-22 plus APAP treated group were presented. (B) Total hepatic glutathione was measured at baseline and the different time points post-APAP intoxication, (C) as well as from control, APAP-challenged and IL-22 plus APAP treated mice at 6 h and 24 h post-APAP administration. A comparable glutathione (GSH) depletion was observed between APAP (400 mg/kg) treatment and IL-22 plus APAP treatment group. Data are expressed as mean ± SEM, *p* value was calculated by un-paired Student's *t* test in B and C, **p* < 0.05, ****p* < 0.001.

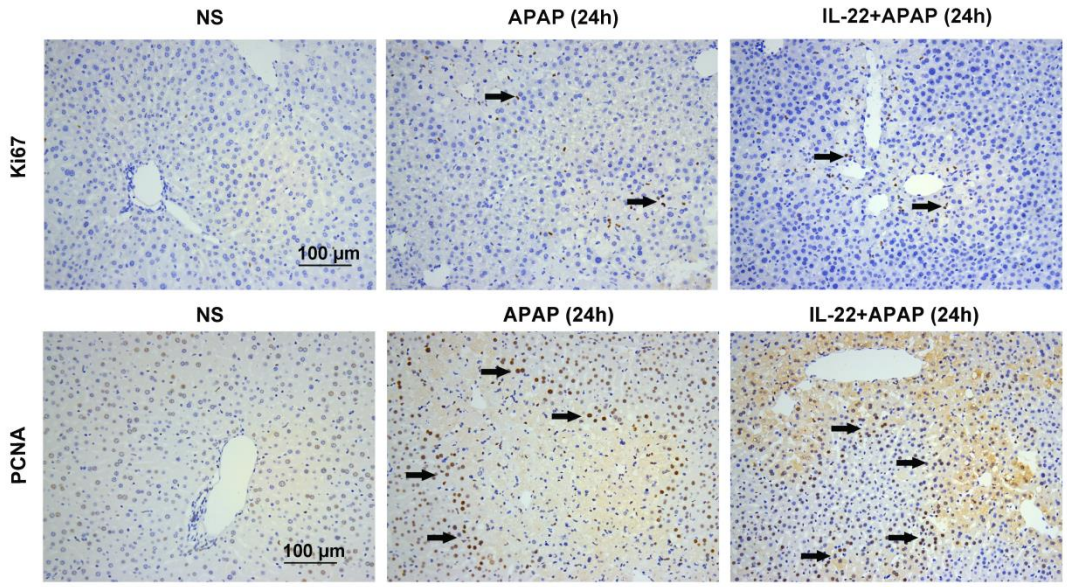

Supplementary Figure 4. Ki-67 and PCNA expression in mice liver tissues.

Representative liver sections images of Ki-67 and PCNA staining from normal control (saline), APAP (400 mg/kg), IL-22 (1 mg/kg) plus APAP (400 mg/kg) treated mice at 24 h after APAP challenged.

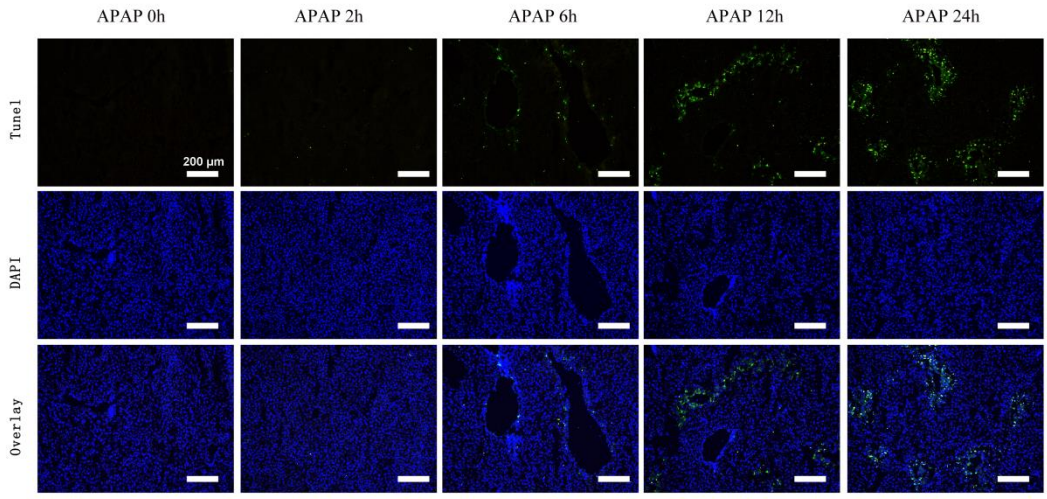

Supplementary Figure 5 Mice liver tissues were subjected to TUNEL staining post-APAP challenged

Hepatic TUNEL staining was performed at various time points after mice challenged with APAP, nuclei were counterstained with DAPI (original magnification 100×).

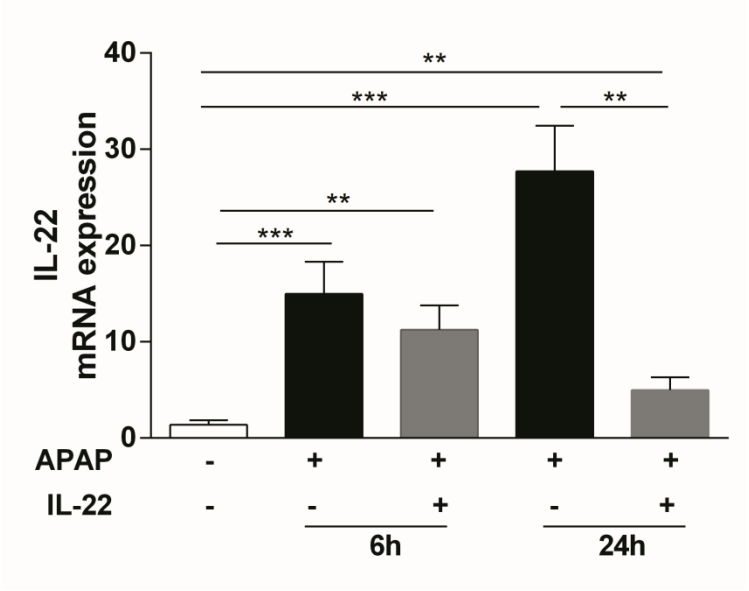

Supplementary Figure 6. Hepatic IL-22 mRNA expression in mice from three experimental groups as indicated.

Hepatic IL-22 mRNA expression was detected in normal control, APAP-challenged and IL-22 plus APAP treated mice at 6 h and 24 h. Data are presented as means ± SEM, *p* value was calculated by Kruskal-Wallis test, ** $p < 0.01$ and *** $p < 0.001$.

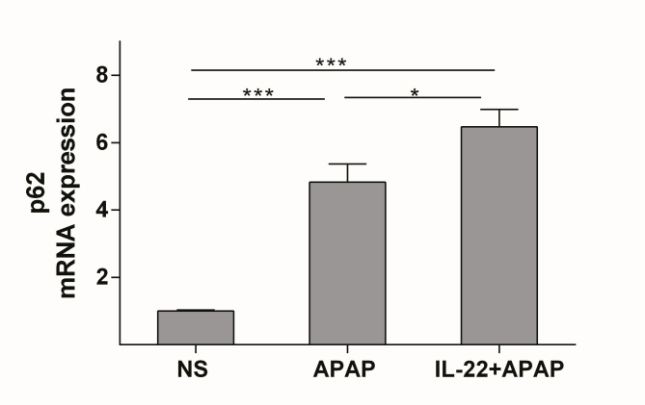

Supplementary Figure 7. IL-22 pretreatment increases hepatic p62 mRNA expression.

Hepatic p62 mRNA expression was detected from three experimental groups at 24 h after APAP challenged. Data are presented as means ± SEM, *p* value was calculated by Kruskal-Wallis test, *$p < 0.05$, *** $p < 0.001$.

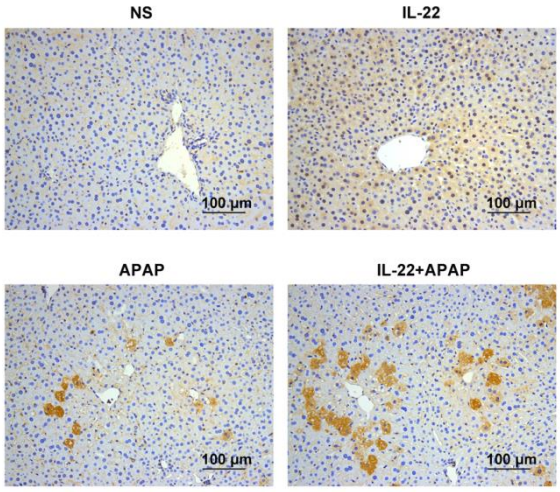

Supplementary Figure 8. Cleaved LC3 expression in mice liver tissues.

Representative liver sections images of cleaved LC3 staining from normal control (saline), IL-22 (1 mg/kg), APAP (400 mg/kg), IL-22 (1 mg/kg) plus APAP (400 mg/kg)

treatment mice at 6 h after APAP challenged.

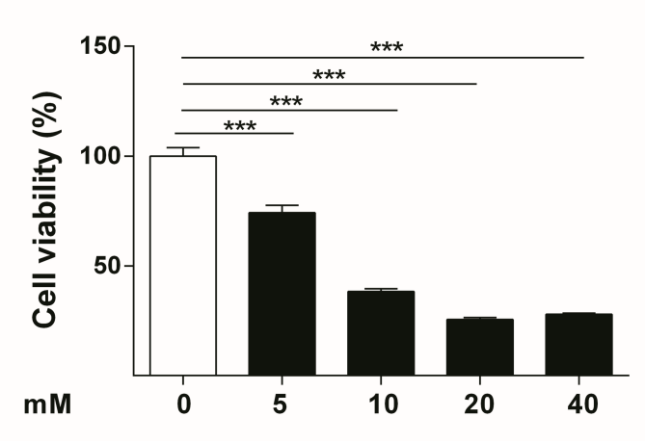

Supplementary Figure 9. APAP exhibits concentration-dependent inhibition of cell viability of L02 cells.

The cell viability of L02 cells was measured after treatment with 5-40 mM of APAP for 24 h. Data are presented as means ± SEM, *p* value was calculated by Kruskal-Wallis test, *** $p < 0.001$.

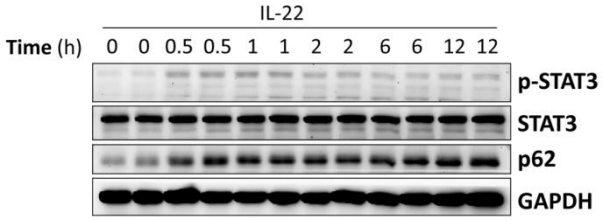

Supplementary Figure 10. IL-22 up-regulates p-STAT3, p62 protein expression in L02 cells.

L02 cells were treated with IL-22 (400 ng/ml) for various periods as indicated, western blot analysis showing p-STAT3, STAT3, p62 expression in L02 cells.

Reference

1. An F, Gong B, Wang H, Yu D, Zhao G, Lin L, Tang W, et al. miR-15b and miR-16 regulate TNF mediated hepatocyte apoptosis via BCL2 in acute liver failure. Apoptosis. 2012; 17: 702-16.
2. Scheiermann P, Bachmann M, Goren I, Zwissler B, Pfeilschifter J, Muhl H. Application of interleukin-22 mediates protection in experimental acetaminophen-induced acute liver injury. Am J Pathol. 2013;182:1107-1113.
3. Ni HM, Boggess N, McGill MR, Lebofsky M, Borude P, Apte U, Jaeschke H, et al. Liver-specific loss of Atg5 causes persistent activation of Nrf2 and protects against acetaminophen-induced liver injury. Toxicol Sci. 2012;127:438-450.
4. Lundback P, Lea JD, Sowinska A, Ottosson L, Furst CM, Steen J, Aulin C, et al. A novel high mobility group box 1 neutralizing chimeric antibody attenuates drug-induced liver injury and postinjury inflammation in mice. Hepatology. 2016;64:1699-1710.
5. Lu Z, Liu J, Liu X, Huang E, Yang J, Qian J, Zhang D, et al. MiR-15a/16-1 Suppresses AHR-dependent IL-22 Secretion in CD4(+) T cells and Contributes to Immune-mediated Organ Injury. Hepatology. 2018; 67: 1027-40.
6. Mo R, Wang P, Lai R, Li F, Liu Y, Jiang S, Zhao G, et al. Persistently elevated circulating Th22 reversely correlates with prognosis in HBV-related acute-on-chronic liver failure. J Gastroenterol Hepatol. 2017;32:677-686.
7. Liu L, Xue Y, Zhu Y, Xuan D, Yang X, Liang M, Wang J, et al. Interleukin 37 limits monosodium urate crystal-induced innate immune responses in human and murine models of gout. Arthritis Res. Ther 2016;18:268.
8. Ni HM, Bockus A, Boggess N, Jaeschke H, Ding WX. Activation of autophagy protects against acetaminophen-induced hepatotoxicity. Hepatology 2012;55:222-232.
9. Lai R, Xiang X, Mo R, Bao R, Wang P, Guo S, Zhao G, et al. Protective effect of Th22 cells and intrahepatic IL-22 in drug induced hepatocellular injury. J Hepatol. 2015;63:148-155.
10. Ahmed MM, Wang T, Luo Y, Ye S, Wu Q, Guo Z, Roebuck BD, et al. Aldo-keto reductase-7A protects liver cells and tissues from acetaminophen-induced oxidative stress and hepatotoxicity. Hepatology. 2011;54:1322-1332.
11. Whelan KA, Merves JF, Giroux V, Tanaka K, Guo A, Chandramouleeswaran PM, Benitez AJ, et al. Autophagy mediates epithelial cytoprotection in eosinophilic oesophagitis. Gut. 2017; 66: 1197-207.
12. N'Diaye EN, Kajihara KK, Hsieh I, Morisaki H, Debnath J, Brown EJ. PLIC proteins or ubiquilins regulate autophagy-dependent cell survival during nutrient starvation. EMBO Rep. 2009;10:173-179.
13. Wang L, Zhang S, Cheng H, Lv H, Cheng G, Ci X. Nrf2-mediated liver protection by esculentoside A against acetaminophen toxicity through the AMPK/Akt/GSK3beta pathway. Free Radic Biol Med. 2016;101:401-412.
14. Wang F, Zhang X, Wang J, Chen M, Fan N, Ma Q, Liu R, et al. LGR4 acts as a link between the peripheral circadian clock and lipid metabolism in liver. J Mol Endocrinol. 2014;52:133-143.
15. Furuta K, Yoshida Y, Ogura S, Kurahashi T, Kizu T, Maeda S, Egawa M, et al. Gab1 adaptor protein acts as a gatekeeper to balance hepatocyte death and proliferation during acetaminophen-induced liver injury in mice. Hepatology. 2016;63:1340-1355.